Electronic Research Archive

http://www.aimspress.com/journal/era

ERA, 33(11): 6742–6770.
DOI: 10.3934/era.2025298
Received: 27 June 2025
Revised: 21 October 2025
Accepted: 27 October 2025
Published: 14 November 2025

Research article

Topological structure determines integration quality and retrieval efficiency

Lei Yang[1], **Honghui Zhang**[2,*] **and Zhongkui Sun**[1,*]

[1] School of Mathematics and Statistics, Northwestern Polytechnical University, Xi'an 710129, China
[2] MIIT Key Laboratory of Dynamics and Control of Complex Systems, Northwestern Polytechnical University, Xi'an 710129, China

* **Correspondence:** Email: haozhucy@nwpu.edu.cn, dynsun@126.com.

Abstract: The hippocampus in the brain encodes memorized information as long-term memory through the plasticity of the CA3–CA1 synaptic network, thereby forming stable engrams. Based on the hippocampal CA3–CA1 synaptic network model, memory engrams are encoded as trajectories within a stable heteroclinic network, where saddle points signify different information blocks. This stable heteroclinic network is further refined into a knowledge network that illustrates the relationships between information blocks, defining the retrieval efficiency, capability, and integration quality of the network among these blocks. In this paper, we examined the impact of the local and global topological properties of the knowledge network on retrieval efficiency, capability, and integration quality. Numerical results indicated that the retrieval efficiency between any two information blocks in the knowledge network decreased with the out-degree of the cue's corresponding node, increased with the in-degree of the target's corresponding node, and was negatively correlated with the distance between node pairs. The retrieval capability of any information block was determined by the out-degree centrality and out-closeness of the corresponding node, while the integration quality of the knowledge network was influenced by the information blocks corresponding to nodes with higher degree centrality or betweenness centrality, and was negatively correlated with the average path length of the network.

Keywords: synaptic network; knowledge network; retrieval efficiency; integration quality

1. Introduction

Memory is the glue that holds our mental life together. Without its unifying power, our conscious and unconscious life would be broken into as many fragments as there are seconds in the day [1]. The neural basis of memory is the engram neurons, which are clusters of neurons in the brain responsible for storing memories [2]. When memories are formed, specific clusters of neurons are activated, and plastic changes occur, including alterations in synaptic strength and the creation of new synaptic

connections, thereby establishing memory engrams. Among the many brain regions involved in memory formation and storage, the hippocampus is irreplaceable in the encoding, consolidation, and retrieval processes of memory, such as contextual memory and spatial memory, due to its unique neural structure and function [3, 4]. The hippocampus is in the temporal lobe of the brain and is divided into the CA1, CA2, CA3, CA4, and dentate gyrus (DG) subregions. It is a "relay station" for memory, responsible for converting fleeting sensory information into memories that can be stored long-term [5].

When a memory is activated, the corresponding cluster of engram neurons is selectively engaged. These neurons collaborate through synaptic connections to collectively represent and process information related to the memory. Within the engram neuron cluster, different neurons may encode various aspects of the memory, such as visual, auditory, and emotional information [6, 7]. Through the intricate synaptic connections and interactions among neurons, these aspects of information are synthesized to create a comprehensive representation of the memory event [8]. Furthermore, neuronal clusters will further process memorized information by extracting pertinent background details and associate them with other memories, thereby enhancing the understanding and utilization of these memories [9].

Memory is not a static storage that remains unchanged, but rather a dynamic process that continuously evolves with individual experiences. For instance, following the retrieval of long-term memories, the hippocampus recruits new engram neurons to reconstruct these memories [10]. During this process, neurogenesis is crucial, providing an opportunity for memory updating [11]. In the reconstruction of memory engrams facilitated by neurogenesis, the newly recruited neurons not only consolidate existing memorized information but also create conditions conducive to the integration and fusion of new information [12]. The brain can modify and supplement existing memories based on new experiences and cognition, making the content of memories more aligned with the current reality, thus achieving memory updates and iterations [13]. As new memories are formed and old memories are updated or forgotten, the synaptic networks in the hippocampus undergo dynamic reorganization [14, 15]. New synaptic connections are formed, while some irrelevant or no longer needed synaptic connections may be weakened or eliminated [16]. This dynamic reorganization enables the hippocampus to adapt to the constantly changing environment and experiences, maintaining effective storage and flexible retrieval of memorized information [17].

The brain is a high-energy-consuming organ, with significantly higher material and metabolic costs relative to its body proportion. Brain networks can reduce these costs by altering their organizational structure [18]. In the evolution of the nervous system, brain networks achieve a dynamic balance between minimizing connection costs and maximizing topological efficiency. This trade-off results in topological properties that lie between regularity and randomness, significantly enhancing the brain's overall information processing efficiency while enabling flexible responses to complex environmental demands [19]. Research on human brain networks consistently demonstrates their small-world properties [20, 21], characterized by high clustering coefficients and short path lengths: High clustering coefficients promote the formation of tightly connected functional modules among brain regions, supporting rapid processing and integration of local information [22]; short path lengths ensure efficient global information propagation [23], enabling cross-module collaboration while reducing noise and signal attenuation during communication [19, 24]. Additionally, studies show that the metabolic cost of nodes in brain networks is proportional to their degree, and the

metabolic cost of edges is proportional to the physical distance they span [25]. The small-world properties, which combine high local and global efficiency [26], represent the optimal manifestation of this cost-efficiency balance.

Yang et al. [27] established a hippocampal CA3–CA1 synaptic network model based on the physiological basis of the hippocampal memory process, encoding memory engrams as trajectories in a stable heteroclinic network [28], and defined the retrieval efficiency and integration quality of memory [29]. Based on the above works, we investigate the regulatory mechanisms of the topological properties of knowledge networks on retrieval efficiency and integration quality, and verify the small-world characteristics of the hippocampal synaptic network.

2. Models and methods

The hippocampus is crucial in the process of memory storage, responsible for encoding memorized information into the plastic changes of the CA3–CA1 synaptic network. Specifically, memorized information is input into the brain in the form of sensory stimuli, entering the hippocampus through the entorhinal cortex and the perforant pathway into the dentate gyrus [30]. During the storage process, the dentate gyrus recruits unique clusters of CA3 engram neurons through the mossy fiber pathway, thereby dividing the memorized information into different blocks [11]. These information blocks induce plastic changes in the CA3–CA1 synaptic network and form stable memory engrams. We assume that the knowledge network, composed of memorized information $\xi^\alpha, \alpha = 0, 1, 2, \cdots$ (reflecting associations between distinct information blocks), is stored within the local CA3–CA1 synaptic network, thereby forming stable memory engrams. Based on the CA3–CA1 synaptic network model of retrieval and integration, modifying the topological structure of this knowledge network elucidates its regulatory influence on the efficiency of memory retrieval and the quality of network integration.

2.1. CA3–CA1 synaptic network model

During the processes of memory storage, retrieval, or integration, the reactivation or repetition of the same information block reactivates the engram neurons in the CA3 region that were involved in storing that information block, thereby modifying the plasticity of the local CA3–CA1 synaptic network. The reactivation process of the CA3 engram neurons is contingent upon a disinhibition mechanism [31, 32]. As illustrated in Figure 1, in the hippocampal CA3 region, parvalbumin-expressing basket cells (PV-BCs) exert a short-term depression effect on a specific class of proposed interneurons (INs) [33]. When the unique engram neurons in the CA3 region, which store the initial memory ξ^0, including INs and excitatory neurons (ECs), continue to participate in the storage of subsequent memories ξ^α, the input information activates PV-BCs, which briefly inhibit INs, leading to the disinhibition of INs on ECs [34]. ECs in the CA3 region release the neurotransmitter glutamate, activating the pyramidal neurons (PCs) in the CA1 region via Schaffer collateral, which temporarily enhances their excitability [5, 35]. Following the cessation of information input, the PV-BCs in the CA3 region gradually silence, enabling INs to release the neurotransmitter GABA once again, which inhibits the ECs in the CA3 region and indirectly reduces the excitability of PCs in the CA1 region [36], thereby maintaining the stability of the memory engram. In simpler terms, memory storage or retrieval temporarily increases the excitability of PCs in the CA1 region through the

disinhibition mechanism in the CA3 region, effectively opening the "engram allocation window" and permitting modifications to the memory engram stored within the local CA3–CA1 synaptic network.

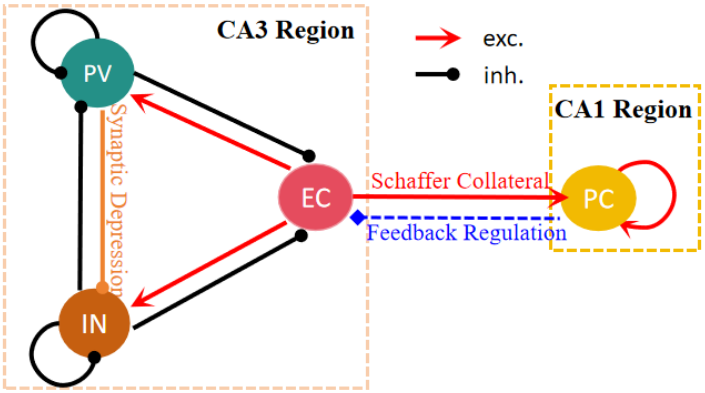

Figure 1. Memory storage or retrieval opens the "engram allocation window". Excitatory cells (EC) in the CA3 region, along with two types of interneurons (PV and IN), form a disinhibition motif, characterized by a short-term synaptic depression mechanism between the PVs and INs. Input information activates the PVs in the CA3 region, which then short-term inhibit the INs, resulting in the disinhibition of the ECs. This leads to the release of neurotransmitters that activate the pyramidal neurons (PCs) in the CA1 region via the Schaffer collateral, thereby opening the engram allocation window and facilitating the modification of memory engrams. Once the input information ceases, the PVs become inactive, and the INs release GABA neurotransmitters to inhibit the ECs in the CA3 region, thereby reducing the excitability of the PCs in the CA1 region, which maintains the stability of memory engrams.

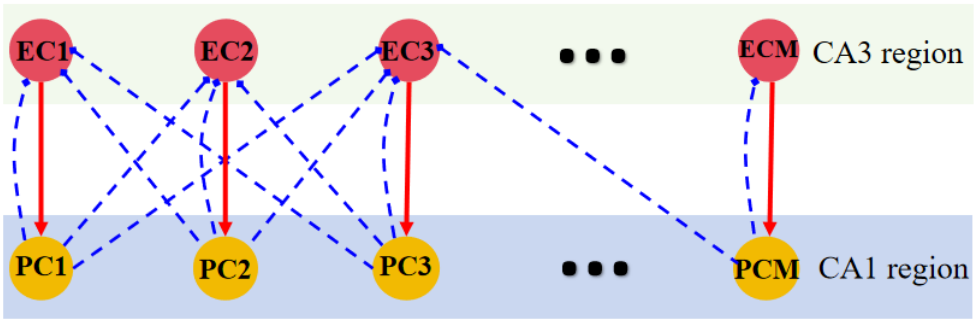

Figure 2. Consider a synaptic network involving CA3 and CA1 regions, consisting of M excitatory neurons (ECs) in the CA3 region and M pyramidal neurons (PCs) in the CA1 region. The dentate gyrus selectively recruits specific CA3 ECs, delivering one-to-one excitatory modulation to CA1 PCs (red arrows), while CA1 PCs exert regulatory influence on CA3 ECs through feedback connections (blue square arrows).

The intensity of the excitatory regulation of CA1 PCs by the disinhibition motif of the CA3 region is contingent upon the inhibitory strength of CA3 INs on ECs. To simplify the network, we consider a CA3–CA1 synaptic network composed of CA3 ECs and CA1 PCs, assuming a one-to-one regulatory relationship from CA3 ECs to CA1 PCs [27]. Furthermore, it is important to note that during short-term memory processes, the efficacy of AMPA receptors on CA1 PCs promotes early long-term potentiation (LTP) of the synapses formed between CA3 ECs and CA1 PCs through positive feedback. Conversely, during long-term memory processes, a negative feedback mechanism inhibits the synthesis of AMPA receptors and induces late LTP. Consequently, we may postulate the existence of a reverse projection from CA1 PCs to CA3 ECs mediating this intricate feedback mechanism [27]. Based on these assumptions, we examine a CA3–CA1 synaptic network composed of M CA3 ECs and M CA1 PCs, as illustrated in Figure 2, which can execute related memory storage tasks. Each CA1 PC within this synaptic network receives indirect feedback regulation from an average of N CA1 PCs, where $N \ll M$, indicating sparse connectivity.

During the process of storing memories $\xi^\alpha, \alpha = 0, 1, 2, \cdots$, the DG recruits specific clusters of engram neurons in the CA3 region, enabling presynaptic ECs to receive tetanic stimulation S_i^α at a frequency of f^α. This stimulation induces calcium transients $P^\alpha(t)$ in postsynaptic PCs, which are mediated by NMDA receptors, with a maximum value fixed at ΔC_N. The spontaneous activity of PCs is characterized as background stimulation V_i at a frequency of k, while the induced calcium transients are denoted as $Q(t)$, mediated by voltage-dependent calcium channels (VDCC), with a maximum value fixed at ΔC_V. Consider the synaptic network model of the hippocampal CA3–CA1 region [27] :

$$\tau_A \frac{dA_i(t)}{dt} = A_i(t)\Big[\sigma_i \cdot H_0(B_i) + \sum_{j=1}^{N} \Theta_j(t)\rho_{ji} H_1(A_j) - \delta_i\Big], \tag{2.1}$$

$$\tau_B \frac{dB_i(t)}{dt} = k_1 B_i^2 - k_2 B_i^3 - k_3 B_i + k_4 C_i, \tag{2.2}$$

$$\frac{dC_i(t)}{dt} = P(t) + Q(t) - S_0(B_i)C_i - \gamma_i(C_i - C_0), i = 1, 2, \cdots, M, \tag{2.3}$$

where $H_0(B_i) = \frac{(B_i/h_0)^{n_0}}{1+(B_i/h_0)^{n_0}}$, $H_1(A_j) = \frac{(A_j/h_1)^{n_1}}{1+(A_j/h_1)^{n_1}}$, $S_0(B_i) = \frac{a_0 B_i}{1+e^{10(B_i-\hat{B}_0)}}$. $C_i(t)$ in Eq (2.3) denotes the concentration of calcium ions in the PC, with the resting calcium concentration represented by C_0. Additionally, γ_i signifies the self-recovery rate of calcium ion concentration. In Eq (2.2), $B_i(t)$ indicates the phosphorylation level of CaMKII in the PC during short-term memory processes, as well as the activation level of the PKC cascade during long-term memory processes. In Eq (2.1), $A_i(t)$ denotes the efficacy of phosphorylated AMPA receptors on the postsynaptic density (PSD) of the PC, while δ_i signifies the dephosphorylation rate of AMPA receptors. Additionally, $\sigma_i H_0(B_i)$ represents the gain of CaMKII cascade or PKA cascade on A_i. The term ρ_{ij} indicates the indirect coupling strength between the i-th PC and the j-th PC, which is determined by the excitatory synaptic coupling strength η_{ii} from the CA3 region EC to the CA1 region PC in a one-to-one manner, as well as the feedback regulation strength ζ_{ji} from the CA1 PC to the CA3 EC. The function $\Theta_j(t) = sgn(\theta_L - \max C_j)$ reflects the nature of the feedback regulation of postsynaptic PCs on presynaptic ECs. When the calcium concentration in the j-th postsynaptic PC is low, $\Theta_j(t) = +1$, indicating a positive feedback effect during the short-term memory process. Conversely, when the maximum calcium concentration exceeds the threshold θ_L, $\Theta_j(t) = -1$, indicating a negative feedback process during the long-term memory process. $\tau_A > \tau_B > 1$ represents the time scales for changes in $A_i(t)$ and $B_i(t)$.

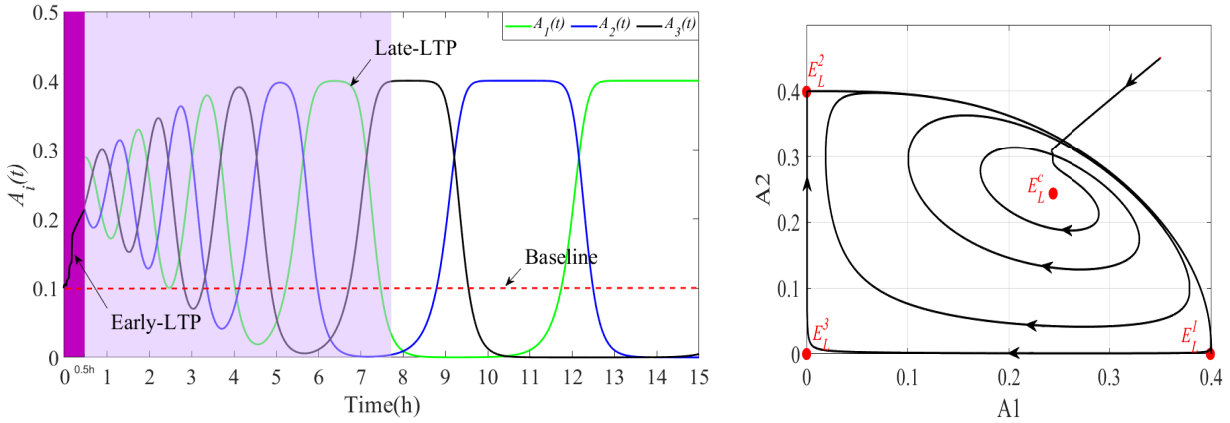

(a) Short-term memory consolidated into long-term memory

(b) Long-term memory encoded into heteroclinic orbits

Figure 3. The dynamic trajectories of $A_i(t)$ during short- and long-term memory processes. (a) When applying four trains of tetanic stimulation S_i, early-LTP is induced (purple shadow), where the Eq (2.1) demonstrates that $\Theta(C_i) = +1$, signifying a short-term memory process. Once the tetanic stimulation S_i ceases, late-LTP is induced (light purple shadow), with $\Theta(C_i) = -1$, indicating a long-term memory process. (b) Throughout the long-term memory process, a stable memory engram is established, exhibiting stable heteroclinic trajectories in the phase space of Eq (2.1), with the trajectory sequentially visiting the saddle points E_L^1, E_L^2 and E_L^3. Figure 3(b) is referenced from [27].

Based on Eq (2.1), when $\Theta(C_i) = -1$, let $F(B_i) = \sigma_i \cdot H_0(B_i) - \delta_i$, which represents the net gain of PKA cascade on the efficacy of AMPA receptors. Let $A_j = 0, j \neq i$, then there exists a unique $A_i^* \in (0, 1)$ such that $F(B_i) = \rho_{ii} H_1(A_i^*), i = 1, 2, \cdots$. Thus, $Q_i : A_i = A_i^*, A_j = 0, j \neq i$ is the equilibrium point of Eq (2.1), with eigenvalues of $-A_i^* \rho_{ii} H_1'(A_i^*) < 0$ and $F(B_j) - \frac{\rho_{ji}}{\rho_{ii}} F(B_i), j \neq i$. When there exists a $j \neq i$ such that $\rho_{ii} F(B_j) - \rho_{ji} F(B_i) > 0$, the equilibrium point Q_i is classified as a saddle point. The theoretical analysis demonstrates that the necessary condition for the existence of stable heteroclinic orbits between these saddle points is the asymmetry of the mutual regulation strength between postsynaptic PCs [28], specifically, $\beta = \frac{\rho_{ij} - \rho_{ii}}{\rho_{ii} - \rho_{ji}} > 1$. After the memory $\xi^\alpha (\alpha = 0, 1, 2, \cdots)$ is consolidated into long-term memory, a stable memory engram is established. In the phase space of Eq (2.1), the memory engram is encoded as trajectories within stable heteroclinic channels [28], as illustrated in Figure 3(b).

3. Knowledge network

3.1. Retrieval efficiency and integration quality

Memory $\xi^\alpha (\alpha = 0, 1, 2, \cdots)$ is stored as long-term memory and forms stable memory engrams. After that, it is represented as heteroclinic trajectories in the phase space of Eq (2.1), where the saddle point set represents different information blocks '$N_0, N_1, N_2, \cdots$'. The non-zero coordinate values of the saddle points are defined as the memory strength of these information blocks, that is,

$$S_{N_i} = \{A_i^* | F(B_i) = \rho_{ii} H_1(A_i^*)\}, i = 1, 2, \cdots . \tag{3.1}$$

According to model (2.1), the retrieval process is characterized as a trajectory originating from the saddle point associated with the cue, which sequentially traverses the saddle points linked to all information blocks along the stable heteroclinic orbits. The process of memory integration is conceptualized as the association of newly acquired knowledge with the pre-existing heteroclinic network through the saddle points corresponding to the repeated information blocks.

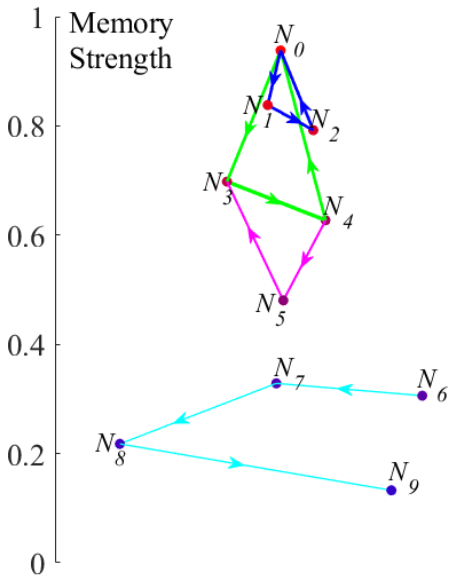

Figure 4. During the storage of the information sequence '$N_0N_1N_2 \times (9)/N_0N_3N_4 \times (6)/N_3N_4N_5 \times (5)/N_6N_7N_8N_9 \times (3)$', the information chunks $N_0N_1N_2$, $N_0N_3N_4$, $N_3N_4N_5$, and $N_6N_7N_8N_9$, which are repeatedly processed, are stored as long-term memories to generate stable memory engrams. In the knowledge network, nodes represent information blocks $N_0, \cdots, N_9$, and directed edges N_iN_j indicate the sequence relationships between information blocks N_i and N_j, as modified from [29].

The stable heteroclinic network is further refined into a knowledge network that illustrates the relationships among all information blocks '$N_0, N_1, N_2, \cdots$', as depicted in Figure 4. The nodes $N_i, i = 0, 1, \cdots$ within the network represent distinct information blocks, and their weights are defined as the memory strength of each information block, specifically, $\omega_{N_i} = S_{N_i}$ [29]. The heteroclinic orbits connecting saddle points are refined into directed edges between nodes, which signify the sequential relationships among information blocks. The weight of the directed edge N_iN_j ($\omega_{N_iN_j}$) is defined as the positive eigenvalue corresponding to the saddle point of the originating node N_i, i.e.,

$$\omega_{N_iN_j} = F(B_j) - \frac{\rho_{ji}}{\rho_{ii}} F(B_i) > 0, i = 1, 2, \cdots, \tag{3.2}$$

making it easier to retrieve information blocks pointed to by directed edges with larger weights [29].

In the knowledge network comprised of information blocks $N_0, N_1, \cdots, N_n$ ($n \geq 1$), a threshold θ_E is introduced. When the weight $\omega_{N_iN_{i+1}}$ of any directed edge along the path exceeds θ_E, the path is deemed valid, otherwise, it is considered invalid. The retrieval efficiency $E(N_0 \cdots N_m)$ ($m \geq 1$) of the valid path

from the clue N_0 to the target N_m, represented as $N_0 \to N_1 \to \cdots N_m$, is defined as the reciprocal of the sum of the products of the reciprocals of all directed edge weights encountered from N_0 to N_m and the exponential function a^x, i.e.,

$$E(N_0 \cdots N_m) = b/\sum_{i=1}^{m} \frac{a^i}{\omega_{N_{i-1}N_i}}, \tag{3.3}$$

where a^x has a base $a > 1$, which indicates the growth rate of retrieval time as the number of nodes increases, and $b > 0$ represents the scale factor.

Based on the definition of retrieval efficiency (3.3), the retrieval capability $F(N_0)$ of node N_0, that is, the ability to retrieve other information blocks in the knowledge network with the information block N_0 as the clue, is defined as

$$F(N_0) = \sum_{i=1}^{n} \hat{E}(N_0 \cdots N_i), \tag{3.4}$$

where $\hat{E}(N_0 \cdots N_i)$ represents the retrieval efficiency corresponding to the optimal retrieval path for retrieving N_i with N_0 as the clue. If this path does not exist, then $\hat{E}(N_0 \cdots N_i) = 0$.

The integration quality $Q(N_0, N_1, \cdots, N_n)$ of a knowledge network composed of information blocks $N_0, N_1, \cdots, N_n$ $(n \geq 1)$ is defined as the average of the product of the retrieval capability $F(N_i)$ of all nodes and the weight ω_{N_i} of that node, that is,

$$Q(N_0, N_1, \cdots, N_n) = \frac{1}{n+1} \sum_{i=0}^{n} \omega_{N_i} F(N_i). \tag{3.5}$$

3.2. *Topological properties of knowledge networks*

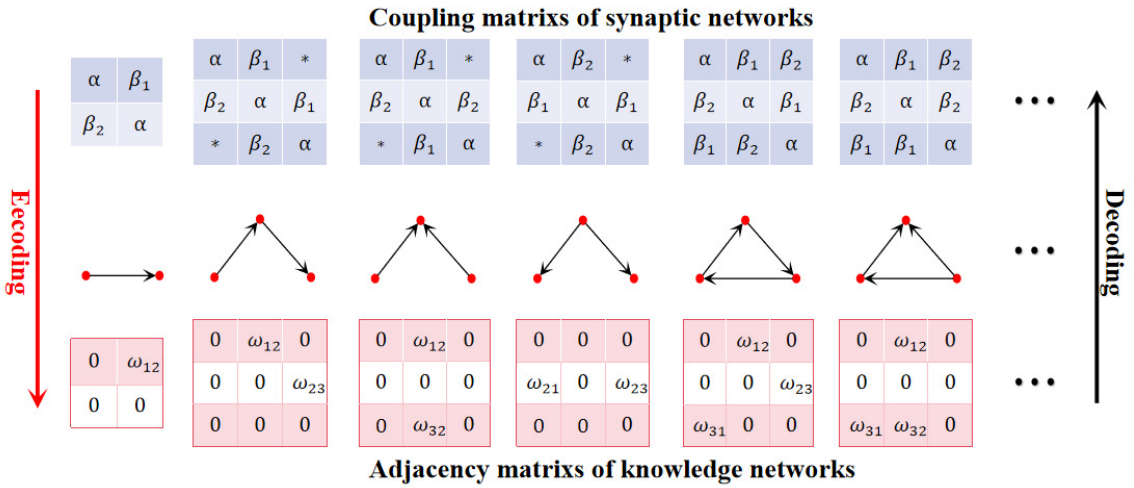

Figure 5. Based on the CA3–CA1 synaptic network model, the hippocampus encodes memories into a knowledge network by regulating the coupling matrix of the synaptic network. The coupling relationships of the synaptic network can be decoded through the adjacency matrix of the knowledge network. In the coupling matrix, $* > \beta_1 > \alpha > \beta_2$ signifies the indirect coupling strength between postsynaptic PCs, while $\omega_{ij}(i, j = 1, 2, 3)$ in the adjacency matrix denotes the weights of directed edges.

In the process of memory storage, the hippocampus modifies the plasticity of the CA3–CA1 synaptic network to encode memories $\xi^{\alpha}, \alpha = 0, 1, \cdots$ as long-term memory, with the memory engrams represented in the form of a knowledge network. Utilizing the CA3–CA1 synaptic network models (2.1)–(2.3), the coupling matrix of the synaptic network can be converted into the adjacency matrix of the knowledge network, as illustrated in Figure 5. General principles of memory storage, such as the observation that information blocks with a higher frequency of repetition exhibit greater memory strength and are more readily retrievable [29], are also manifested in the knowledge network through an increased weighting on the nodes and directed edges. Subsequently, based on the definitions of retrieval efficiency (3.3) and integration quality (3.5) discussed earlier, we examine the influence of topological properties of the knowledge network on the retrieval efficiency among information blocks and the overall quality of network integration.

In the knowledge network composed of nodes $N_0, N_1, \cdots, N_n$ ($n \geq 1$) representing information blocks, the degree of any node N_i is given by

$$D(i) = D^{in}(i) + D^{out}(i), i = 0, 1, \cdots, n,$$

where the in-degree $D^{in}(i)$ represents the number of directed edges pointing to node N_i, and the out-degree $D^{out}(i)$ represents the number of directed edges originating from node N_i. The average degree of the knowledge network is

$$D_{avg} = \frac{1}{n+1} \sum_{i=0}^{n} D(i),$$

and the degree distribution $p(k)$ represents the probability that a randomly selected vertex has a degree of k. The distance $L(i, j)$ between node N_i and N_j is defined as the minimum number of edges that must be traversed to get from clue N_i to target N_j. If there is no path from N_i to N_j, then $L(i, j) = +infty$. The average path length of the network is defined as

$$L_{avg} = \frac{1}{n(n+1)} \sum_{i=0}^{n} \sum_{j=0}^{n} L(i, j).$$

The clustering coefficient is a measure of a network or node's tendency to form clusters or closely connected communities. In the directed network, the clustering coefficient of node N_i is defined as the ratio of the number of directed edges between its neighbors to the total possible edges among these neighbors, expressed mathematically as

$$C(i) = \frac{e_{out}(i) + e_{in}(i)}{D^{out}(i)(D^{out}(i) - 1) + D^{in}(i)(D^{in}(i) - 1)}.$$

Here, $D^{out}(i)$ and $D^{in}(i)$ denote the out-degree and in-degree of the node N_i, respectively, while $e_{out}(i)$ and $e_{in}(i)$ indicate the number of directed edges connecting the out-neighbors and in-neighbors of that node. The average clustering coefficient of the network is calculated as

$$C_{avg} = \frac{1}{n+1} \sum_{i=0}^{n} C(i).$$

First, consider several types of regular networks, such as star networks, tree networks, circular networks, and complete networks, which have unique topological properties [37, 38]. As shown in

Figure 6(a), the divergent star network formed by $n + 1$ nodes has a unique central node with an out-degree of n, and the in-degrees of the remaining n edge nodes are all 1. The path length from the central node to the edge nodes is 1, and the clustering coefficient of all nodes is 0. The degree distribution of tree networks is also uneven (Figure 6(b)), with the root node having an out-degree 2, branch nodes having an out-degree of 2 and an in-degree of 1, and leaf nodes possessing an in-degree of 1. The distance from the root node to other nodes is equal to the height h of that node, and the clustering coefficient of any node is also 0. In the circular network, the in-degree and out-degree of each node are both 1, the average path length is $\frac{n+1}{2}$, and the clustering coefficient of each node is 0, as shown in Figure 6(c). As the control group, in the complete graph (Figure 6(d)), the in-degree and out-degree of each node are n, the clustering coefficient is also 1, and the average path length between all nodes is 1. By structuring the knowledge network into these types of regular networks, we examine the influence of local properties, such as out-degree, in-degree, and clustering coefficient, on the retrieval efficiency among information blocks.

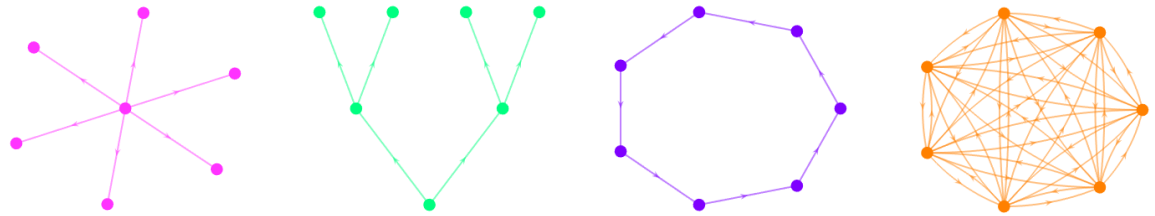

(a) Star Network (b) Tree Network (c) Circular Network (d) Complete Network

Figure 6. Several classic network types composed of $n + 1 = 7$ nodes. (a) In a divergent star network, the out-degree of the central node is 6, the in-degree of the edge nodes is 1, the path length from the central node to the edge nodes is all 1, and the clustering coefficient of the nodes is zero. (b) The out-degree of the root node in the tree network is 2, the out-degree of the branch nodes is 2, the in-degree is 1, the in-degree of the leaf nodes is 1. The distance from the root node to the branch nodes is 1, the distance to the leaf nodes is 2, and the clustering coefficient of any node is zero. (c) In a circular network, the in-degree and out-degree of each node are both 1, the average path length is 3.5, and the clustering coefficient of the nodes is also zero. (d) Fully connected network, with both the in-degree and out-degree being 6, the degree distribution is uniform, the path length between all nodes is 1, and the clustering coefficient is also 1.

A large amount of evidence indicates that synaptic networks are neither strictly regular nor entirely random, typically displaying small-world characteristics marked by high local and global efficiency, as well as a modular community structure [19]. Consequently, a knowledge network exhibiting small-world properties is constructed based on the Watts-Strogatz (W-S) model, which incorporates 'centrality' metrics, including degree centrality, betweenness centrality, and closeness centrality. By systematically removing nodes with differing centralities from the knowledge network, the global properties of the network are modified, enabling the assessment of changes in retrieval capability and integration quality among information blocks within the knowledge network. This approach explores

the influence of the local topological characteristics of nodes on retrieval capability and global topological characteristics of the knowledge network on integration quality.

4. Numerical results

Next, during the numerical simulation process, we consider a knowledge network comprised of $n + 1$ information blocks. By transforming the knowledge network into a regular network, we analyze the effects of local properties, such as the out-degree, in-degree, and clustering coefficient of nodes within the knowledge network, on the retrieval efficiency among information blocks. Subsequently, a knowledge network exhibiting small-world properties is constructed using the Watts-Strogatz (W-S) model. We examine the 'centrality' of nodes and modify the degree distribution, average path length, and average clustering coefficient of the knowledge network through node deletion, thereby assessing the impact of these global properties on the integration quality of the knowledge network.

Based on the topological structure of the knowledge network, we decode the indirect coupling matrix of the synaptic network $\{\rho_{ij}\}$, as well as the net gain in the efficacy of AMPA receptors resulting from PKA cascade within PCs, denoted as $F(B_i)$. Subsequently, we calculate the retrieval efficacy and capablity of nodes and the integration quality of the knowledge network, thereby elucidating the influence of network topological properties on these factors. In a knowledge network, a node's degree is directly proportional to the frequency with which the information block has been reiterated, leading to an enhanced net gain $F(B_i)$ of the PKA cascade on AMPA receptor efficacy. Consequently, we define $F(B_i)$ as a function of the degree $D(i)$ of the corresponding node associated with the information block, i.e.,

$$F(B_i) = \frac{2}{\pi}\arctan(D(i)), i = 0, 1, \cdots, n. \tag{4.1}$$

During the memory storage process, the coupling strength η_{ii} of the excitatory synapses between CA3 ECs and ca1 PCs increases as a result of short-term or long-term potentiation of synaptic plasticity. Moreover, as the number of repetitions of the information block increases, the coupling strength of the synapses responsible for storing that information block becomes stronger, which is defined as $\eta_{ii} = 2 - exp(-\sqrt{D(i)})$. In the context of long-term memory, due to the inhibitory effects of the CA3 disinhibition motif on the CA1 PCs, the indirect coupling strength ρ_{ji} between CA1 PCs monotonically decreases with respect to η_{ii} and the negative feedback strength ζ_{ji}. Therefore, we can posit that the indirect coupling strength ρ_{ji} between PCs is

$$\rho_{ji}(D(i)) = \frac{1}{\eta_{ii}(D(i))\zeta_{ji}} = \frac{1}{[2 - exp(-\sqrt{D(i)})]\zeta_{ji}}, i, j = 0, 1, \cdots, n. \tag{4.2}$$

After being stored as long-term memory, we let the self-feedback strength of the CA1 PC that store the information block be $\zeta_{ii} = 0.5$, and the asymmetric feedback regulation strength between the two PCs be $\zeta_{ij} = 0.3 < \zeta_{ii} < \zeta_{ji} = 1$, resulting in asymmetry $\beta > 1$, and a heteroclinic orbits between saddles Q_i and Q_j. Consequently, there exists a directed edge N_iN_j between nodes N_i and N_j.

4.1. Regular networks

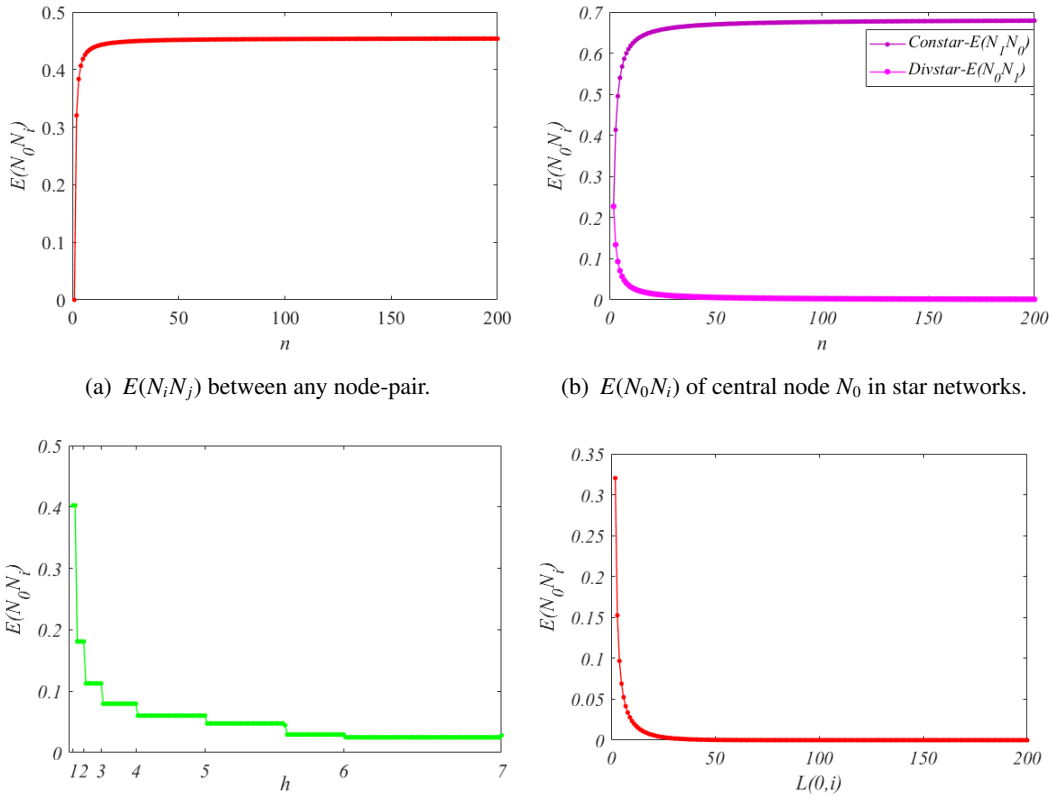

(a) $E(N_iN_j)$ between any node-pair.

(b) $E(N_0N_i)$ of central node N_0 in star networks.

(c) $E(N_0N_i)$ of the root node N_0in tree network.

(d) $E(N_0N_i)$ of node N_0 in a directed circular network.

Figure 7. The retrieval efficiency $E(N_iN_j)$ between node-pairs of the network under different network structures. (a) In a complete network, the properties of all nodes are consistent, and the retrieval efficiency $E(N_0N_i)$ of any node (such as N_0) to other nodes (N_i) monotonically increases with the network size n and approaches the saturation value $b/2a$. (b) In a convergent star network, all edge nodes N_i point to the central node N_0, and the retrieval efficiency $E(N_iN_0)$ of N_i to N_0 increases monotonically with the in-degree $D^{in}(0) = n$ of the central node N_0, approaching $\frac{3b}{4a}$. In a divergent star network, directed edges go from the central node N_0 to the edge nodes N_i, the retrieval efficiency $E(N_0N_i)$ of N_0 to N_i decreases monotonically with the out-degree $D^{out}(0) = n$ of the central node N_0, approaching zero. (c) In a directed tree network, the distance $L(0, i)$ from the root node N_0 to other nodes N_i is equal to the height h of that node. The retrieval efficiency $E(N_0N_i)$ of the root node N_0 for branch nodes or leaf nodes N_i decreases monotonically with the distance h. (d) In a directed circular network, the retrieval efficiency $E(N_0N_i)$ of node N_0 for other nodes N_i exhibits a monotonic decrease as the distance $L(0, i)$ increases.

As a control group, in a complete network comprising $n + 1$ nodes, the out-degree and in-degree of any node are n, and the distance between any two nodes is 1, as illustrated in Figure 6(d). Utilizing the information block associated with node N_0 as a clue, the retrieval efficiency for the information blocks

corresponding to other nodes N_i is

$$E(N_0N_i) = \frac{b\arctan(2n)}{\pi a}.$$

Consequently, the retrieval efficiency $E(N_iN_j)$ of any node-pairs within a knowledge network characterized by a fully connected structure increases with the scale n of the network, and tend to the saturation value $\frac{b}{2a}$, as shown in Figure 7(a).

In a divergent star network consisting of $n + 1$ nodes, the central node N_0 has an out-degree of $D^{out}(0) = n$ and an in-degree of zero, while the other edge nodes $N_i, i = 1, 2, \cdots$ have an in-degree of 1 and an out-degree of zero, as shown in Figure 6(a). When retrieving the information block corresponding to the edge node N_i employing the central node N_0 as a clue, the retrieval efficiency

$$E(N_0N_i) = \frac{2b}{\pi a}[\arctan(1) - 0.5\arctan(n)] > 0,$$

decreases as the out-degree of the nodes increases, approaching zero. Similarly, in a converging star network (that is, all directed edges point from edge nodes to the central node), the efficiency of retrieving the information block corresponding to the central node N_0 using the edge node N_i as a clue, i.e.,

$$E(N_iN_0) = \frac{2b}{\pi a}[\arctan(n) - 0.5\arctan(1)] > 0,$$

increases with the in-degree of the central node $D^{in}(0) = n$ and approaches a fixed value of $\frac{3b}{4a}$, as shown in Figure 7(b). Consequently, the following conclusion may be drawn.

Corollary 4.1. *During the retrieval process, the larger the out-degree $D^{out}(i)$ of the clue corresponding node N_i, the lower the retrieval efficiency $E(N_iN_j)$. Conversely, the larger the in-degree $D^{in}(i)$ of the target corresponding node N_j, the greater the $E(N_iN_j)$.*

In a tree network with $n + 1$ nodes, the root node N_0 has an out-degree of k and an in-degree of zero. The branch nodes have an out-degree of k and an in-degree of 1, while the leaf nodes have an out-degree of zero but an in-degree of 1, as shown in Figure 6(b). When retrieving the information block corresponding to the branch node N_i at l-th (where $l \geq 1$) layer, utilizing the information block associated with the root node N_0 as a clue, the efficiency of retrieval is

$$E(N_0N_i) = \frac{2b}{\pi a}\frac{(a-1)\omega_0\omega_1}{(a-1)\omega_1 + a(a^{l-1}-1)\omega_0}.$$

The retrieval efficiency when retrieving the information block corresponding to leaf node N_j is

$$E(N_0N_j) = \frac{2b}{\pi a}\frac{(a-1)\omega_0\omega_1\omega_2}{(a-1)(\omega_1\omega_2 + a^{h-1}\omega_0\omega_1) + (a^{h-1}-1)\omega_0\omega_2},$$

where $\omega_0 = \arctan(k+1) - 0.5\arctan(k)$, $\omega_1 = 0.5\arctan(k+1)$, $\omega_2 = \arctan(1) - 0.5\arctan(k+1)$, h represents the height of the tree network, which is the path length $L(0, j)$ from the root node N_0 to the leaf node. The retrieval efficiency of retrieving the $l + m$-th layer branch node N_j with the l-th layer branch node N_i as a clue is

$$E(N_iN_j) = \frac{2b}{\pi a}\frac{(1-a)\omega_1}{1-a^m}.$$

The retrieval efficiency of leaf node N_j is

$$E(N_iN_j) = \frac{2b}{\pi}\frac{(a-1)\omega_1\omega_2}{(a-1)a^{h-l}\omega_1 + a(1-a^{h-l-1})\omega_2}.$$

The greater the distance between the node associated with the retrieved information block and the node corresponding to the clue, the lower the retrieval efficiency, as illustrated in Figure 7(c).

In a counterclockwise circular network comprising $n+1$ nodes, each node N_i has an out-degree and in-degree of 1, and the average path length is expressed as $L_{avg} = \frac{n+1}{2}$, as illustrated in Figure 6(c). When retrieving other information blocks N_i using the information block associated with node N_0 as a clue, the retrieval efficiency is

$$E(N_0N_i) = \frac{b(a-1)}{\pi a}\frac{\arctan(2)}{a^{L(0,i)}-1},$$

here, $L(0,i)$ denotes the distance between node N_i and N_0. Revalidate that the retrieval efficiency $E(N_0N_i)$ decreases as the distance $L(0,i)$ increases, as demonstrated in Figure 7(d). Therefore, it can be inferred from the correlation between retrieval efficiency and distance:

Corollary 4.2. *During the retrieval process, for different paths to retrieve the target information block from the clues, the longer the distance $L(i,j)$, the lower the retrieval efficiency $E(N_iN_j)$.*

From the definition of retrieval efficiency (3.3), it is evident that retrieval efficiency is influenced by the path length from the clue to the target, as well as the weights of the directed edges encountered. Based on the weights of the directed edges (3.2) and Eqs (4.1) and (4.2), in both circular and tree networks, the weights of each directed edge remain consistent. Therefore, retrieval efficiency is determined solely by the path length. Therefore, as the number of information blocks accessed increases (resulting in a longer path), the retrieval efficiency decreases.

To investigate the influence of the clustering coefficient on retrieval efficiency among node-pairs, we utilize converged star networks. By incrementally adding edges between edge nodes, we observe an increase in the local clustering coefficient $C(N_0)$ of the central node N_0, as illustrated in Figure 8(a),(b).

In a converged star network, all edge nodes are incoming nodes of the central node N_0. Based on the definition of the local clustering coefficient $C(i)$, the local clustering coefficient of the central node N_0, $C(N_0) = \frac{e_{in}(N_0)}{n(n-1)}$, increases monotonically with the number of directed edges between edge nodes $e_{in}(N_0)$, as shown in Figure 8(c). However, since changes in $e_{in}(N_0)$ do not affect the distance from edge nodes N_i to the central node N_0 ($L(i,0) = 1$), nor do they change the in-degree ($D^{in}(0) = n$) and out-degree ($D^{out}(0) = 0$) of N_0, the retrieval efficiency $E(N_iN_0)$ of edge nodes N_i for N_0 remains unchanged. From the definition of retrieval efficiency (3.3), it is evident that the retrieval efficiency between node-pairs does not correlate with the local clustering coefficient of the target nodes. Similarly, in a divergent star network, the addition of directed edges between the edge nodes indicates that the retrieval efficiency also exhibits no correlation with the local clustering coefficient of the clue nodes. Therefore,

Corollary 4.3. *During the retrieval process, the retrieval efficiency $E(N_iN_j)$ between the clues and the target information blocks is independent of the clustering coefficient $C(N_i)$ and $C(N_j)$ of the corresponding nodes of the clues and the targets.*

In summary, the discussion regarding the retrieval efficiency of information blocks within directed star, tree, circular, and complete knowledge networks reveals that the retrieval efficiency $E(N_iN_j)$ is

related to the out-degree and in-degree of the clue or target corresponding nodes, as well as the distance between them. In star and complete networks, the distance from node N_0 to other nodes N_i is 1. When N_0 is a clue to retrieve other information blocks, the greater the out-degree of N_0, the lower the retrieval efficiency. Conversely, when N_0 is the target being retrieved, the greater the in-degree of N_0, the easier it is to retrieve it. From the discussion of tree and circular networks, it can be concluded that when the out-degree and in-degree of node N_0 remain constant, the retrieval efficiency $E(N_0N_i)$ for retrieving other nodes N_i corresponding to information blocks decreases monotonically with the distance $L(0, i)$. By modifying the convergent star network, it is observed that adjusting the local clustering coefficient $C(N_0)$ of the central node N_0, while keeping its in-degree and out-degree unchanged, as well as maintaining the distance between it and the edge nodes N_i, results in no variation in $E(N_iN_0)$ or $E(N_0N_i)$. This finding highlights the independence of retrieval efficiency from the local clustering coefficient.

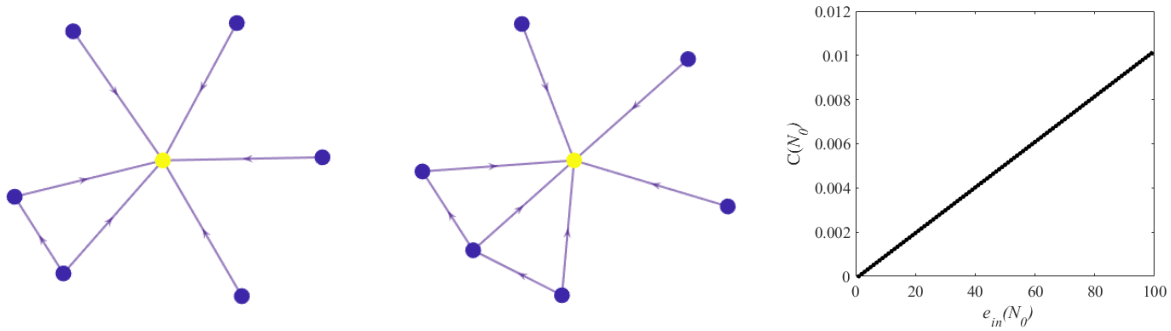

(a) $e_{in}(N_0) = 1$ (b) $e_{in}(N_0) = 2$ (c) Local clustering coefficient $C(N_0)$

Figure 8. (a) and (b) Gradually increasing the number of directed edges among edge nodes $e_{in}(N_0)$ in a converged star network, enhances the clustering coefficient $C(N_0)$ of the central node N_0. (c) As $e_{in}(N_0)$ increases, the clustering coefficient of the central node $C(N_0)$ exhibits a monotonic increase.

By comparing Figure 9(a),(b), it is evident that when the network scale remains consistent, the fully connected structure of the knowledge network, characterized by the shortest average path length and the highest clustering coefficient, demonstrates the greatest integration quality. This is followed by the circular structure and tree structure, while the star structure of the knowledge network exhibits the lowest integration quality. Although the fully connected structure maximizes integration quality, it incurs the cost of dense synaptic connections, which does not conform to the sparse coding strategy observed in brain networks [39, 40]. The circular structure of the knowledge network possesses relatively high integration quality and can be realized through sparse synaptic connections. However, this type of network structure suffers from poor robustness, as the removal of any node or edge significantly diminishes integration quality. Furthermore, as the scale increases, the retrieval efficiency between node pairs within the circular structure of the knowledge network becomes notably low, as illustrated in Figure 7(d). Consequently, after evaluating the integration quality of several regular networks alongside the retrieval efficiency between node pairs, it is determined that the convergent star structure and tree structure of the knowledge network strike a better balance among

integration quality, retrieval efficiency, and the connection cost of the synaptic network, thereby aligning more closely with the organizational principles of brain networks.

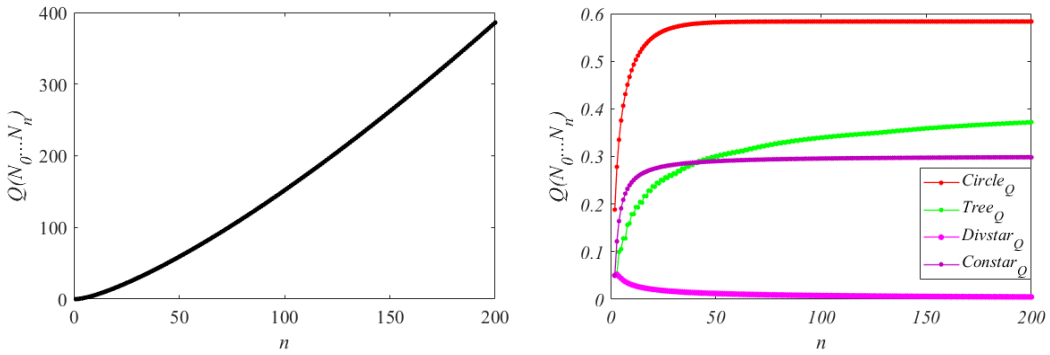

(a) Integration quality in a complete network (b) Integration quality of diverse knowledge networks

Figure 9. The integration quality $Q(N_0 \cdots N_n)$ of the knowledge network varies with the network scale n under different network structures. (a) The $Q(N_0 \cdots N_n)$ of a complete graph is monotonically increasing with respect to the network size n. (b) The $Q(N_0 \cdots N_n)$ of a divergent star network decreases monotonically with the network size n, while the $Q(N_0 \cdots N_n)$ of convergent star networks, directed tree networks, and circular networks increases monotonically with the network size n. At the same scale, the integration quality of directed circular networks is significantly higher than that of other types of networks. The parameters are $a = 1.1$ and $b = 1$.

4.2. Small world network

A small-world directed network containing $n + 1 = 1000$ nodes is constructed based on the Watts-Strogatz (W-S) model, where each node initially has $k/2 = 25$ outgoing and incoming neighbors, and the incoming and outgoing neighbor nodes are reselected with probabilities $p = 0.5$ and $q = 0.5$, respectively. In the formed small-world directed network, the average clustering coefficient is $C_{avg} = 0.06$, the average path length is $L_{avg} = 2.2$, the maximum and minimum retrieval capability of information blocks are $F_{max} = 213.8$ and $F_{min} = 190.5$, and the integration quality of the network is $\hat{Q}(N_0 \cdots N_n) = 494.4$. Next, by calculating the retrieval capabilities of information blocks corresponding to nodes with different clustering coefficients, degree centrality, betweenness centrality, or closeness in this knowledge network, we reveal the impact of local properties of nodes on retrieval capability. By deleting nodes with distinct local characteristics from the network, representing the forgetting of corresponding information blocks, the change in the integrated quality of the network is calculated as $Q_{err} = \frac{Q(i)-\hat{Q}}{maxQ(i)-\hat{Q}}$, where $Q(i)$ denotes the integrated quality of the network after the deletion of node N_i, and $\hat{Q}$ represents the original integrated quality of the network. This method tests the impact of node local characteristics on the integrated quality of the knowledge network.

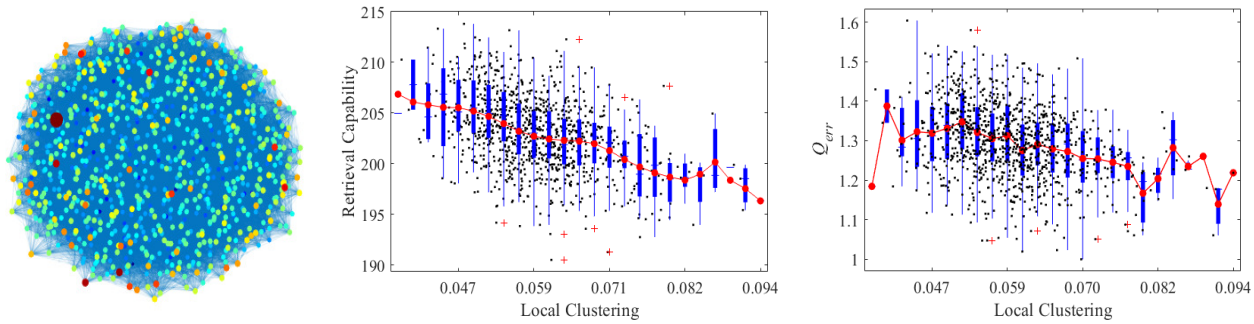

(a) Local clustering coefficient (b) Retrieval capability & Clustering coefficient (c) Integration quality & Clustering coefficient

Figure 10. The local clustering coefficient $C(N_i)$ of node N_i has a negative linear correlation with the retrieval capability $F(N_i)$ of the corresponding information block and the variation of the network integration quality Q_{err}. (a) Schematic diagram of the local clustering coefficient of nodes in a small-world network. (b) The larger the $C(N_i)$ of node N_i, the lower the retrieval capability $F(N_i)$ of the corresponding information block, indicating a negative linear correlation between $F(N_i)$ and $C(N_i)$, with a correlation index of $r = -0.4116$. (c) After deleting node N_i, the change in network integration quality Q_{err} has a weak negative linear correlation with $C(N_i)$, with a correlation coefficient of $r = -0.3111$.

In the small-world network, the maximum and minimum local clustering coefficients are $C_{max} = 0.0952$ and $C_{min} = 0.0365$, respectively, with only a few nodes having a high clustering coefficient, as shown in Figure 10(a). By calculating the local clustering coefficient $C(N_i)$ for each node in the network and the corresponding retrieval capability $F(N_i)$ of the information block, we oberserve that nodes with a larger clustering coefficient $C(N_i)$ have a smaller retrieval capability $F(N_i)$, as illustrated in Figure 10(b). The Pearson correlation coefficient between $F(N_i)$ and $C(N_i)$ is calculated as $r = -0.4116$, $p = 0$, demonstrating a weak negative linear correlation between $F(N_i)$ and $C(N_i)$. After sequentially removing nodes N_i with varying local clustering coefficients from the small-world network, the integration quality Q of the network decreases. However, the extent of the decrease in Q, referred to as Q_{err}, diminishes as $C(N_i)$ of the removed nodes increases. As illustrated in Figure 10(c), the correlation index between these two variables is $r = -0.3111$. From this, we can conclude:

Corollary 4.4. *In the knowledge network composed of nodes $N_0, \cdots, N_n$, the retrieval capability of the information block corresponding to node N_i, denoted as $F(N_i)$, has a weak negative linear correlation with the local clustering coefficient $C(N_i)$ of N_i, while the integration quality $Q(N_0, \cdots, N_n)$ of the network has a weak positive linear correlation with $C(N_i)$.*

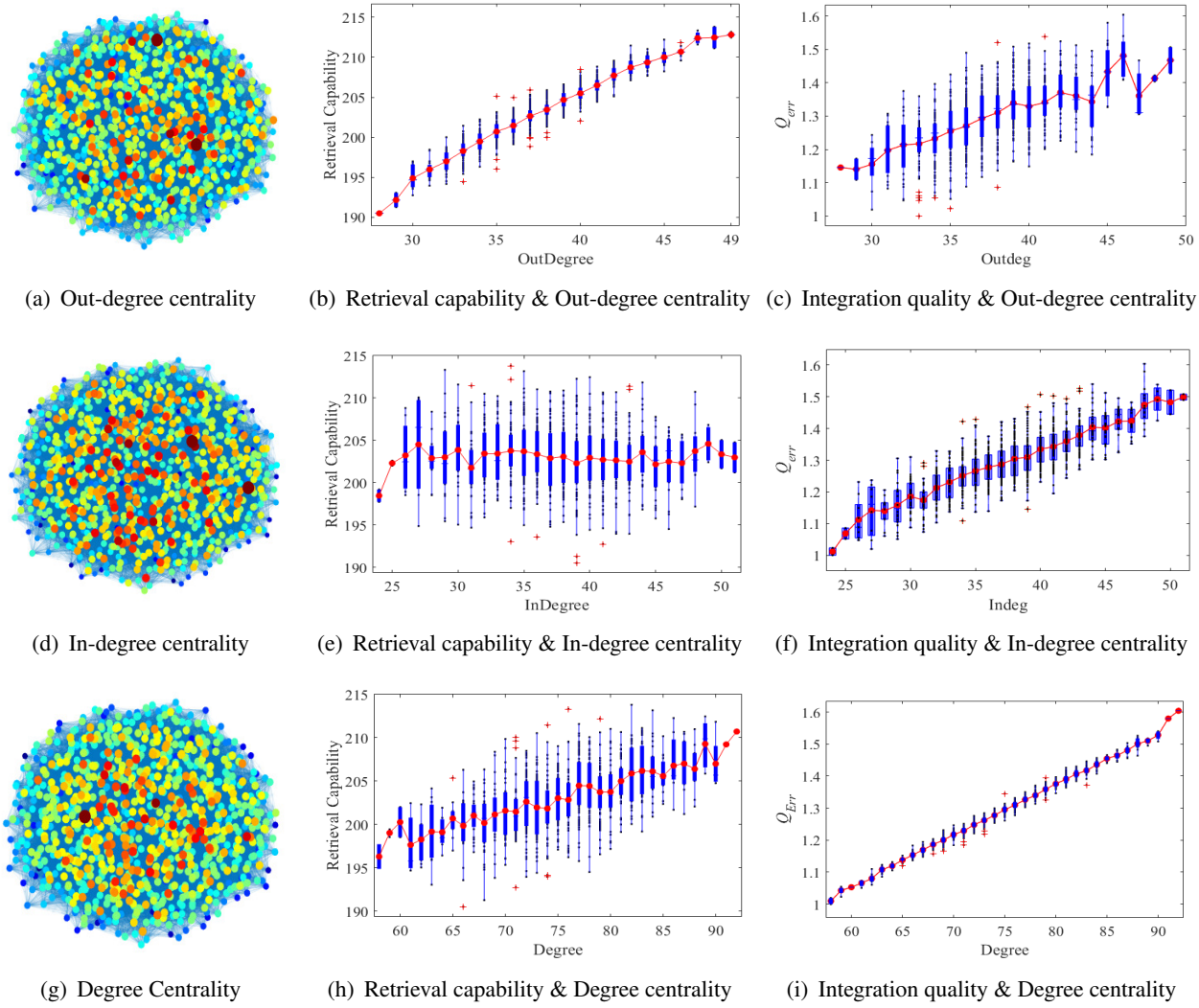

(a) Out-degree centrality (b) Retrieval capability & Out-degree centrality (c) Integration quality & Out-degree centrality

(d) In-degree centrality (e) Retrieval capability & In-degree centrality (f) Integration quality & In-degree centrality

(g) Degree Centrality (h) Retrieval capability & Degree centrality (i) Integration quality & Degree centrality

Figure 11. The retrieval capability $F(N_i)$ of node N_i is closely related to its out-degree centrality $C_{deg}^{out}(i)$. Moreover, the larger the out-degree centrality $C_{deg}^{out}(i)$, in-degree centrality $C_{deg}^{in}(i)$, or degree centrality $C_{deg}(i)$ of the deleted node N_i, the more significantly the integration quality of the network Q decreases. (a) Schematic diagram of the out-degree centrality of nodes in a small-world network. (b) The retrieval capability $F(N_i)$ of the node is significantly positively linearly correlated with its out-degree centrality C_{deg}^{out}, with a correlation coefficient of $r = 0.9464$. (c) After the deletion of the node N_i with $C_{deg}^{out}(N_i)$, the change in the integration quality of the network, denoted as Q_{err}, exhibits a weak positive linear correlation with C_{deg}^{out}, evidenced by a correlation coefficient of $r = 0.5738$. (d) Schematic diagram of the in-degree centrality of nodes in a small-world network. (e) $F(N_i)$ does not have a significant correlation with the node's in-degree centrality C_{deg}^{in}, with a Pearson correlation coefficient of $r = -0.0474, p = 0.1342$. (f) Q_{err} has a significant positive linear correlation with C_{deg}^{in}, with a correlation coefficient of $r = 0.794$. (g) Schematic diagram of degree centrality of nodes in a small-world network. (h) $F(N_i)$ has a weak positive linear correlation with the node's degree centrality $C_{deg}(i)$, with a correlation coefficient of $r = 0.5173$. (i) Q_{err} has a significant positive linear correlation with C_{deg}, with a correlation coefficient of $r = 0.9909$.

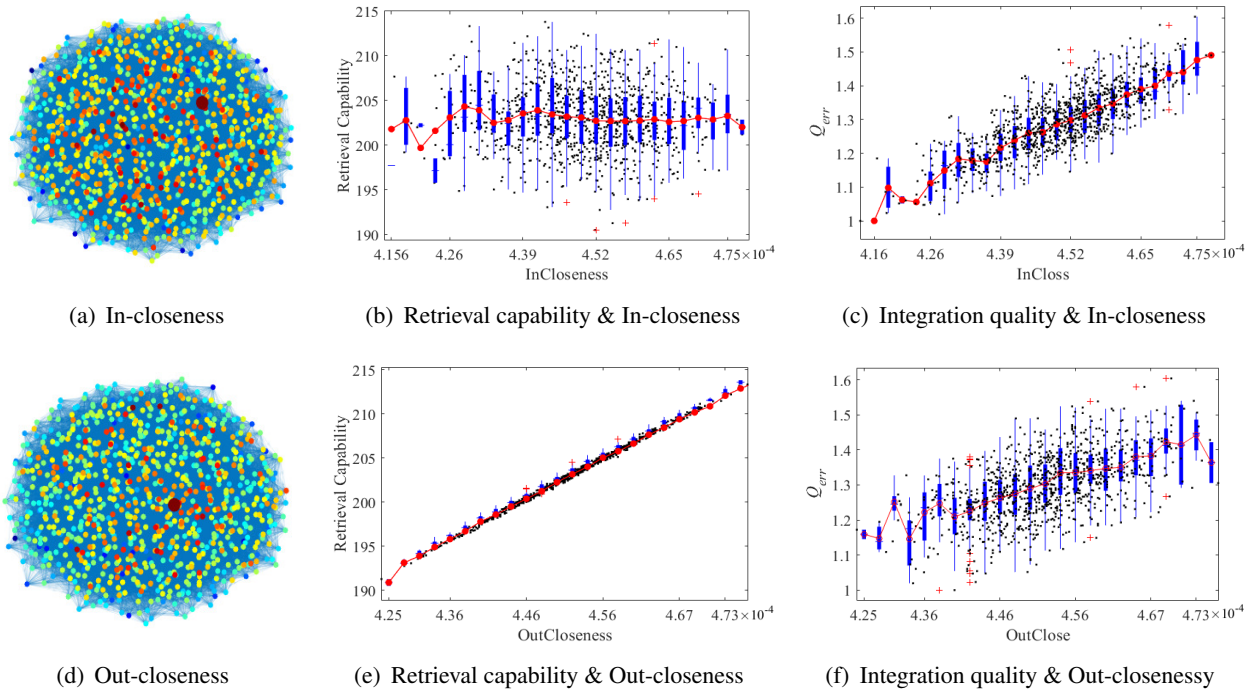

(a) In-closeness (b) Retrieval capability & In-closeness (c) Integration quality & In-closeness

(d) Out-closeness (e) Retrieval capability & Out-closeness (f) Integration quality & Out-closenessy

Figure 12. The retrieval capability $F(N_i)$ of nodes N_i with a larger out-closeness $C_{clo}^{out}(i)$ is greater, while the influence of nodes N_i with a larger in-closeness $C_{clo}^{in}(i)$ on the integration quality Q of the network is also greater. (a) Schematic diagram of the in-closeness C_{clo}^{in} in a small-world network. (b) $F(N_i)$ of node N_i has no correlation with its in-closeness $C_{clo}^{in}(i)$, with a Pearson correlation coefficient of $r = -0.0448$, $p = 0.1573$. (c) The larger the $C_{clo}^{in}(i)$ of the deleted node N_i, the greater the decrease in integration quality Q_{err}. That is, there is a strong positive linear correlation between Q_{err} and C_{clo}^{in}, with a correlation coefficient of $r = 0.7822$. (d) Schematic diagram of the out-closeness C_{clo}^{out} in a small-world network. (e) $F(N_i)$ of node N_i has a significant positive linear correlation with its out-closeness $C_{clo}^{out}(i)$, with a correlation coefficient of $r = 0.9986$. (f) There exists a weak positive linear correlation between the C_{clo}^{out} of the deleted node N_i and Q_{err}, with a correlation coefficient of $r = 0.5501$.

The degree centrality of a node is a metric that highlights highly connected nodes. In a directed graph, the degree centrality $C_{deg}(i)$ of any node N_i can be decomposed into out-degree centrality $C_{deg}^{out}(i) = D^{out}(i)$ and in-degree centrality $C_{deg}^{in}(i) = D^{in}(i)$. In the established small-world network, the maximum degree centrality is $C_{deg}(738) = 94$, which includes $C_{deg}^{out}(738) = 46$ and $C_{deg}^{in}(738) = 48$, as shown in Figure 11(a),(d),(g). The numerical results indicate that the retrieval capability $F(N_i)$ of node N_i exhibits a strong positive linear correlation with $C_{deg}^{out}(N_i)$ ($r = 0.9464$), and a weaker positive linear correlation with C_{deg} ($r = 0.5173$). Conversely, no correlation was found with C_{deg}^{in} ($p = 0.1342$), as illustrated in Figure 11(b),(e),(h). Following the sequential deletion of nodes N_i, Q_{err} demonstrates a positive linear correlation with the C_{deg}^{out}, C_{deg}^{in}, and C_{deg} of the deleted node N_i. As depicted in Figure 11(c),(f),(i), the correlation coefficients are $r = 0.5738$, 0.794, and 0.9909, respectively. This finding suggests that the higher the degree centrality or in-degree centrality of the deleted node, the more pronounced the decline in network integration quality. Consequently, the following inference may be drawn:

Corollary 4.5. *In the knowledge network composed of nodes $N_0, \cdots, N_n$, a node N_i with a higher degree centrality $C_{deg}(i)$ or in-degree centrality $C^{in}_{deg}(i)$ contributes significantly to the overall integration quality $Q(N_0, \cdots, N_n)$ of the network. Additionally, a node N_i with a greater out-degree centrality $C^{out}_{deg}(i)$ demonstrates enhanced retrieval capability $F(N_i)$ for the information block associated with that node.*

The closeness of a node can identify nodes within the network that are capable of communicating swiftly with other nodes. The out-closeness of any node N_i is defined as the reciprocal of the sum of distances from that node to all other nodes, specifically,

$$C^{out}_{clo}(i) = \frac{1}{n}\frac{A_i}{L_i},$$

where A_i represents the number of nodes reachable from node N_i, and L_i denotes the sum of distances from node N_i to all reachable nodes. The closeness of a directed graph is further categorized into out-closeness and in-closeness, as shown in Figure 12(a),(d). For in-closeness, L_i is defined as the sum of distances from all other nodes to N_i. In a knowledge network characterized by a small-world structure, Pearson correlation analysis revealed that the retrieval capability $F(N_i)$ of the information block corresponding to any node N_i is not correlated with the node's in-closeness $C^{in}_{clo}(i)$ ($r = -0.0448$), but is significantly positively linearly correlated with its out-closeness $C^{out}_{clo}(i)$ ($r = 0.9986$), as illustrated in Figure 12(b),(e). By examining the correlation between the change in integration quality Q_{err} following the deletion of nodes and the $C^{out}_{clo}(i)$ and $C^{in}_{clo}(i)$ of the removed nodes, it is determined that the integration quality Q exhibits a strong correlation with the node's in-closeness $C^{in}_{clo}(i)$ ($r = 0.7822$) but a weaker correlation with its out-closeness $C^{out}_{clo}(i)$ ($r = 0.5501$), as depicted in Figure 12(c),(f). In conclusion, the following insights can be drawn regarding the out-closeness and in-closeness of nodes:

Corollary 4.6. *In a knowledge network composed of information blocks $N_0, \cdots, N_n$, nodes with a higher out-closeness $C^{out}_{clo}(i)$ correspond to stronger retrieval capability $F(N_i)$ of the information block N_i while having a weaker impact on the integration quality Q of the network. On the other hand, the in-closeness $C^{in}_{clo}(i)$ of a node does not affect its retrieval capability $F(N_i)$ but has a significant impact on the integration quality Q of the network.*

Betweenness centrality quantifies the frequency with which a node appears on the shortest paths connecting two other nodes within the network, as illustrated in Figure 13(a). Since there may be multiple shortest paths between two nodes N_s and N_t, the betweenness centrality of node N_i is given by

$$C_{bet}(i) = \sum_{s,t \neq i} \frac{n_{st}(i)}{N_{st}},$$

where $n_{st}(i)$ is the number of shortest paths from node N_s to N_t that pass through node N_i, and N_{st} is the total number of shortest paths from node N_s to N_t. Pearson correlation analysis reveals a weak positive linear correlation between $F(N_i)$ of the information block corresponding to node N_i and its betweenness centrality $C_{bet}(i)$, with a correlation coefficient of $r = 0.5458$, as shown in Figure 13(b). However, after the removal of node N_i, the decrease in the integration quality Q of the network, denoted as Q_{err}, monotonically increases with $C_{bet}(i)$, showing a significant positive linear correlation, with a

correlation coefficient of $r = 0.9858$, as depicted in Figure 13(c). This indicates that the integration quality Q of the network has a significant negative linear correlation with the betweenness centrality $C_{bet}(i)$ of the nodes, leading to the inference:

Corollary 4.7. *In a knowledge network composed of information blocks $N_0, \cdots, N_n$, a node N_i with a higher betweenness centrality $C_{bet}(i)$ contributes more significantly to the integration quality $Q(N_0 \cdots N_n)$ of the network.*

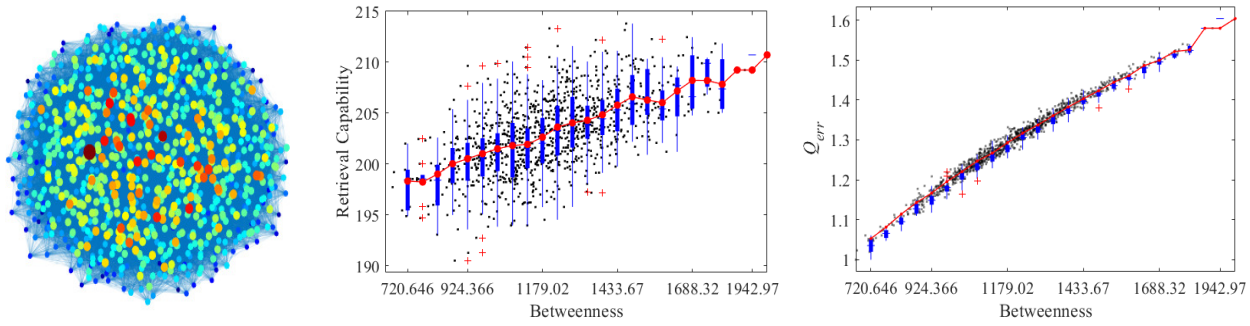

(a) Betweenness centrality (b) Retrieval capability & Betweenness centrality (c) Integration quality & Betweenness centrality

Figure 13. The retrieval capability $F(N_i)$ of node N_i has a weak positive correlation with betweenness centrality $C_{bet}(i)$, but there is a significant positive linear correlation with integration quality Q. (a) Schematic diagram of the betweenness centrality $C_{bet}(i)$ of nodes in a small-world network. (b) $F(N_i)$ of node N_i has a weak positive linear correlation with its betweenness centrality $C_{bet}(i)$, with a correlation coefficient of $r = 0.5458$. (c) The greater the $C_{bet}(i)$ of the deleted node N_i, the greater the reduction in Q_{err}, indicating a significant positive linear correlation between them ($r = 0.9858$).

In small-world networks, the removal of any node alters the global properties of the network, including the global clustering coefficient and the average path length, while affecting the retrieval capability of information blocks and the integration quality of the network. Numerical results indicate that in a knowledge network composed of nodes $N_0, \cdots, N_n$, there is no significant linear correlation between the global clustering coefficient C_{avg} and the change in integration quality Q_{err} or the retrieval capability of the deleted node $F(N_i)$, as illustrated in Figure 14(a),(b), with Pearson correlation coefficients of $r = 0.1988$ and $r = -0.0886$, respectively. However, a linear correlation exists between the average path length L_{avg} and both $F(N_i)$ and Q_{err}, particularly a significant positive linear correlation between Q_{err} and L_{avg}, with a correlation coefficient of $r = 0.9858$, as shown in Figure 14(c),(d). Therefore, the following inference can be drawn:

Corollary 4.8. *In the knowledge network composed of nodes $N_0, \cdots, N_n$, the integration quality $Q(N_0 \cdots N_n)$ exhibits a monotonically decreasing trend in relation to the average path length L_{avg}, and it remains independent of the global clustering coefficient C_{avg}. The linear correlation between the retrieval capability $F(N_i)$ of the information block associated with any node N_i and L_{avg} is weak, whereas the correlation with C_{avg} can be considered negligible.*

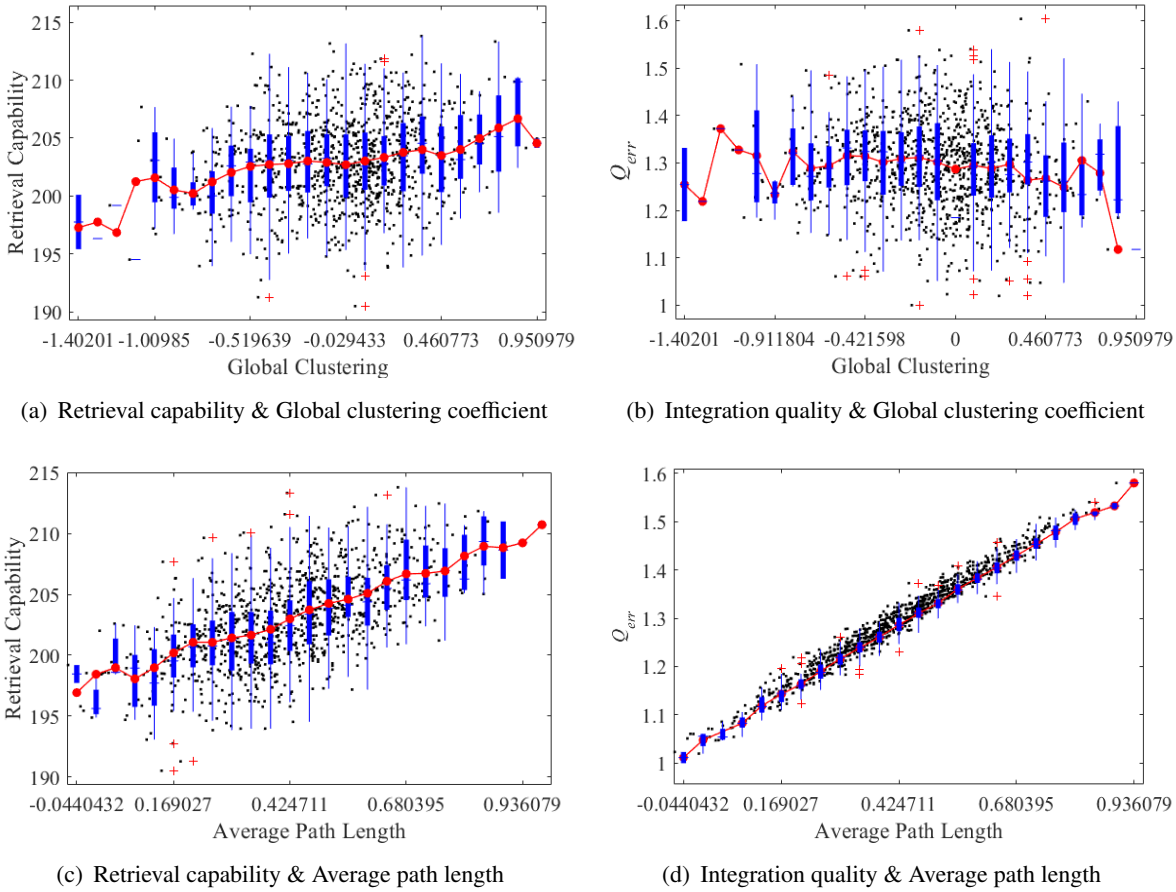

(a) Retrieval capability & Global clustering coefficient

(b) Integration quality & Global clustering coefficient

(c) Retrieval capability & Average path length

(d) Integration quality & Average path length

Figure 14. The correlation between the global clustering coefficient C_{avg} or average path length L_{avg} of the network after deleting node N_i and the retrieval capability $F(N_i)$ or the decrease in network integration quality Q_{err}. (a) There is no significant correlation between $F(N_i)$ of the deleted node N_i and C_{avg}, with a Pearson correlation coefficient of $r = 0.1988$. (b) There is no significant correlation between C_{avg} and Q_{err}, with a correlation coefficient of $r = -0.0886$. (c) $F(N_i)$ of the deleted node N_i has a weak positive linear correlation with L_{avg}, with a correlation coefficient of $r = 0.5681$. (d) After deleting node N_i, there is a significant positive linear correlation between L_{avg} and Q_{err}, with a correlation coefficient of $r = 0.9858$.

In the knowledge network characterized by the small-world structure, an analysis of the retrieval capability $F(N_i)$ of the information block corresponding to node N_i, alongside its Pearson correlation coefficients with various local properties (refer to Table 1), reveals a highly significant positive linear correlation between $F(N_i)$ with the out-degree centrality $C_{deg}^{out}(i)$ and out-closeness $C_{clo}^{out}(i)$ of node N_i. $F(N_i)$ exhibits a monotonically increasing linear relationship with both $C_{deg}^{out}(i)$ and $C_{clo}^{out}(i)$, while showing no correlation with the in-degree centrality $C_{deg}^{in}(i)$ and in-closeness $C_{clo}^{in}(i)$ of node N_i. Additionally, other local properties of node N_i, such as the local clustering coefficient $C(i)$, degree centrality $C_{deg}(i)$, and betweenness centrality $C_{bet}(i)$, exert only a minimal influence on $F(N_i)$ of the corresponding information block, without playing a decisive role. Consequently, $F(N_i)$ of node N_i in the network is primarily determined by its out-degree centrality $C_{deg}^{out}(i)$ or out-closeness $C_{clo}^{out}(i)$.

By systematically removing nodes N_i with varying local properties within the network, we examine the influence of both the local attributes of node N_i and the global characteristics of the network on the integration quality $Q(N_0, \cdots, N_n)$. For convenience, we discuss the correlation between the decrease in normalized integration quality Q_{err} and the local properties of node N_i, and calculate the Pearson correlation coefficient, as detailed in Table 1. It is found that Q_{err} has a significant positive linear correlation with the degree centrality $C_{deg}(i)$ and betweenness centrality $C_{bet}(i)$ of the deleted node N_i, indicating a significant negative linear correlation between the integration quality $Q(N_0, \cdots, N_n)$ and the degree centrality $C_{deg}(i)$ and betweenness centrality $C_{bet}(i)$ of the nodes. Although other local properties of the deleted node N_i also show positive or negative linear correlations with Q_{err}, they are not as significant as the degree centrality $C_{deg}(i)$ and betweenness centrality $C_{bet}(i)$. Additionally, the correlation between the average path length of the network L_{avg} and Q_{err} is also very significant. Therefore, the integration quality of the knowledge network $Q(N_0, \cdots, N_n)$ is determined by the nodes with higher degree centrality $C_{deg}(i)$ and betweenness centrality $C_{bet}(i)$, as well as the future average path length L_{avg}.

Table 1. The Pearson correlation coefficients of the global clustering coefficient C_{avg}, average path length L_{avg}, retrieval capability $F(N_i)$, and the reduction of integration quality Q_{err} with respect to the local properties of deleted nodes.

	C_{avg}	L_{avg}	$F(N_i)$	Q_{err}
Local clustering coefficient	[-0.8464, 0]	[-0.3958, 0]	[-0.4116, 0]	[-0.3111, 0]
Out-degree centrality	[0.0747, 0.0182]	[0.5669, 0]	[0.9464, 0]	[0.5738, 0]
In-degree centrality	[-0.2589, 0]	[0.7552, 0]	[-0.0474, 0.1342]	[0.7940, 0]
Degree centrality	[-0.1692, 0]	[0.9549, 0]	[0.5173, 0]	[0.9909, 0]
In-closeness	[-0.1732, 0]	[0.7711, 0]	[-0.0448, 0.1573]	[0.7822, 0]
Out-closeness	[0.2121, 0]	[0.5765, 0]	[0.9986, 0]	[0.5501, 0]
Betweenness centrality	[-0.0280, 0.3763]	[0.9846, 0]	[0.5458, 0]	[0.9900, 0]
Global clustering coefficient	[−, −]	[−, −]	[0.1988, 0]	[-0.0886, 0.0051]
Average path length	[−, −]	[−, −]	[0.5681, 0]	[0.9858, 0]

5. Discussion

Memory, as a fundamental pillar of cognitive systems, not only encompasses an individual's life experiences and knowledge reserves but also serves as the foundation for learning, decision-making, and social interaction. Efficient retrieval of memory is essential for our adaptation to the environment and the advancement of cognitive development. The hippocampal CA3–CA1 synaptic network models (2.1)–(2.3) established by Yang et al. [27] elucidates the processes of memory storage, encoding [28], forgetting, retrieval, and integration [29]. Building upon this model, the knowledge acquired through learning induces plastic changes in the synaptic network within the hippocampus, which are stored as long-term memories, with memory engrams encoded as trajectories in stable heteroclinic networks, thereby forming a dynamic knowledge network. This unique encoding method renders the distinctive topological properties of the knowledge network a critical factor influencing the local or global efficiency of memory. Based on the discussion regarding memory retrieval and

integration processes, the retrieval efficiency (3.3) between information blocks and the integration quality (3.5) of the knowledge network are clearly defined [29]. Here, the influence of the topological properties of the knowledge network on the retrieval efficiency, capability of memory and the quality of integration.

In knowledge networks, node degree ($D(i)$) maps the number of repeated activations of information blocks. A higher value indicates a greater net gain of the PKA cascade ($F(B_i)$) within PCs in the synaptic network (Eq (4.1)), as well as stronger synaptic coupling (η_{ii}) between CA3-ECs and CA1-PCs (Eq (4.2)), serving as a core quantitative indicator of memory strength (Eq (3.1)) [41]. The weight of directed edge ($\omega_{N_iN_j}$) corresponds to the stability of heteroclinic orbits between saddle points (defined by positive eigenvalues), relating to the efficiency of electrical signal diffusion. Retrieval is the process of accessing the corresponding saddle points of information blocks, depending on the activation of AMPA receptors on PCs in the synaptic network via electrical signal diffusion [42], closely related to the excitability of PCs and the diffusion distance. Retrieval efficiency (Eq (3.3)) quantifies the speed of cue-target extraction, reflecting AMPA receptor efficacy ($A_i(t)$, which denotes the excitability of PCs) as well as the attenuation characteristics of electrical signals. Retrieval capability (Eq (3.4)) characterizes the associative extraction range of a single information block, corresponding to the activation radiation capacity of specific engram cell clusters. Integration quality (Eq (3.5)), calculated as the weighted average of node weights (memory strength) and retrieval capability, reflects the synergistic efficiency of the knowledge network, corresponding to the dynamic binding of new and old memories by the hippocampal heteroclinic network.

Certain regularly structured network topologies, including star, tree, and ring configurations, exhibit distinctive topological characteristics. Through the discussion of these regular networks, reveals the impact of out-degree, in-degree and distance on the efficiency of retrieving information blocks. Consistent with the conclusions of Sporns [24], shorter path lengths indicate closer physical distances within the synaptic network, and retrieval efficiency is negatively correlated with the distance between the target and the cue (Corollary 4.2). A higher in-degree of the target node implies a higher $F(B_j)$ within the corresponding PC, which increases the efficacy of AMPA receptors, i.e., greater excitability of PCs, resulting in higher retrieval efficiency (Corollary 4.1). This aligns with the general principles of retrieval, where nodes with higher in-degrees imply greater weights of directed edges, making them easier to retrieve, while higher out-degrees indicate more directed edges, meaning more interference with memory and a greater likelihood of retrieval failure.

Brain synaptic networks typically exhibit small-world properties. A knowledge network with small-world properties is constructed using the Watts-Strogatz model to examine the correlation between the retrieval capability of information blocks corresponding to nodes and centralities of those nodes. Through Pearson correlation analysis, it is found that the retrieval capability of information blocks is determined by the out-degree centrality and out-closeness of the corresponding nodes (Corollaries 4.5 and 4.6), meaning that the more information blocks that can be retrieved using the information block corresponding to that node as a clue, the greater the retrieval capability. However, the clustering coefficient of the nodes shows a weak negative linear correlation with the retrieval efficiency of the corresponding information blocks (Corollary 4.4), which may be due to the fact that the retrieval efficiency of information blocks is influenced not only by the topological properties of the network but also by the memory strength of the information blocks (Eq (3.3)).

By removing nodes with different centralities in the network, we examine the extent to which the

quality of integration decreases, finding that nodes with higher degree centrality or betweenness centrality contribute more to the integration quality of the network (Corollaries 4.5 and 4.7). Although the in-degree centrality and in-closeness of nodes also have some impact on integration quality (Corollaries 4.5 and 4.6), they are not decisive factors. Among the global properties of knowledge networks, the integration quality of the network is independent of the clustering coefficient and is determined by the average path length. The shorter the average path length, the greater the integration quality (Corollary 4.8), which is consistent with the findings of Gallos et al. [26]. Furthermore, we did not discuss the impact of network degree distribution on integration quality, as changes in network degree distribution depend on the degree centrality of the deleted nodes. Therefore, it can be inferred that the greater the impact of information blocks corresponding to nodes with higher degree centrality on integration quality, the greater the integration quality of knowledge networks with heavy-tailed degree distributions.

Based on our dynamic hippocampal CA3–CA1 synaptic network models (2.1)–(2.3), the adjacency matrix of the knowledge network is not merely a static mapping but a dynamic decoder of the indirect coupling matrix $\{\rho_{ij}\}$ between CA1 pyramidal neurons (Figure 5). This decoding process is inherently adaptive: The directed edges between nodes in the knowledge network, realized through synaptic loops linking engram cells of corresponding information blocks, undergo continuous reorganization as memory engrams are consolidated, retrieved, or forgotten. Consistent with Bullmore and Sporns's findings [19], the knowledge network's requirement for high integration quality (short average path length and heavy-tailed distribution) manifests as a modular small-world structure in the synaptic network. Critically, these modules are not fixed: New memory information, when integrated, expands modules or initiates new ones by strengthening nascent synaptic connections between engram cells, while repeated retrieval of old memories densifies intra-module synapses, dynamically tuning the balance between dense internal connections (within modules) and sparse inter-module links. The dynamic nature of this topology directly supports memory function: High retrieval efficiency between information blocks emerges not from static proximity but from activity-dependent synaptic plasticity, repeated co-activation of cue and target engram cells shortens their effective distance via strengthened intermediate synapses. Similarly, high retrieval capability arises from dynamic regulation of retrograde messengers and synaptic connectivity: Frequent activation enhances postsynaptic release of retrograde signals, expanding the pool of regulated CA1 engram neurons and flexibly boosting cross-module communication when needed. This explains why retrieval efficiency and capability are particularly robust within modules, where synaptic plasticity is most pronounced due to repeated co-activation of related information blocks. In essence, the static topological properties analyzed in this study represent snapshots of an inherently dynamic system, where every node weight, edge strength, and module structure is continuously reshaped by memory processing, aligning with the brain's evolutionary ability to adapt its network architecture to ongoing experiential demands.

Use of AI tools declaration

The authors declare they have not used Artificial Intelligence (AI) tools in the creation of this article.

Acknowledgments

This work was supported by the National Natural Science Foundation of China (Grant Nos. 12472032, 12272295 and 12372064). The authors thank the editors and anonymous reviewers for their comments.

Conflict of interest

The authors declare there are no conflicts of interest.

References

1. E. Kandel, Y. Dudai, M. Mayford, The molecular and systems biology of memory, *Cell*, **157** (2014), 163–186. https://doi.org/10.1016/j.cell.2014.03.001
2. S. Josselyn, S. Tonegawa, Memory engrams: Recalling the past and imagining the future, *Science*, **367** (2020), eaaw4325. https://doi.org/10.1126/science.aaw4325
3. S. Chen, N. Cheng, X. Chen, C. Wang, Integration and competition between space and time in the hippocampus, *Neuron*, **112** (2024), 3651–3664. https://doi.org/10.1016/j.neuron.2024.08.007
4. L. D. Kolibius, S. A. Josselyn, S. Hanslmayr, On the origin of memory neurons in the human hippocampus, *Trends Cognit. Sci.*, **29** (2025), 421–433. https://doi.org/10.1016/j.tics.2025.01.013
5. A. Tzilivaki, J. J. Tukker, N. Maier, P. Poirazi, R. P. Sammons, D. Schmitz, Hippocampal GABAergic interneurons and memory, *Neuron*, **111** (2023), 3154–3175. https://doi.org/10.1016/j.neuron.2023.06.016
6. R. E. Harvey, H. L. Robinson, C. Liu, A. Oliva, A. Fernandez-Ruiz, Hippocampo-cortical circuits for selective memory encoding, routing, and replay, *Neuron*, **111** (2023), 2076–2090. https://doi.org/10.1016/j.neuron.2023.04.015
7. J. W. Chen, C. Zhang, P. Y. Hu, B. Min, L. P. Wang, Flexible control of sequence working memory in the macaque frontal cortex, *Neuron*, **112** (2024), 3502–3514. https://doi.org/10.1016/j.neuron.2024.07.024
8. D. F. Tomé, Y. Zhang, T. Aida, O. Mosto, Y. Lu, M. Chen, et al., Dynamic and selective engrams emerge with memory consolidation, *Nat. Neurosci.*, **27** (2024), 561–572. https://doi.org/10.1038/s41593-023-01551-w
9. Y. M. Zhou, H. W. Zhu, Z. Y. Liu, X. Chen, X. J. Su, C. N. Ma, et al., A ventral CA1 to nucleus accumbens core engram circuit mediates conditioned place preference for cocaine, *Nat. Neurosci.*, **22** (2019), 1986–1999. https://doi.org/10.1038/s41593-019-0524-y
10. R. Refaeli, T. Kreisel, M. Groysman, A. Adamsky, I. Goshen, Engram stability and maturation during systems consolidation, *Curr. Biol.*, **33** (2023), 3942–3950. https://doi.org/10.1016/j.cub.2023.07.042
11. L. Y. Prince, T. J. Bacon, C. M. Tigaret, J. R. Mellor, Neuromodulation of the feedforward dentate gyrus-CA3 microcircuit, *Front. Synaptic Neurosci.*, **8** (2016), 32. https://doi.org/10.3389/fnsyn.2016.00032

12. B. Lei, B. Kang, Y. Hao, H. Yang, Z. Zhong, Z. Zhai, et al., Reconstructing a new hippocampal engram for systems reconsolidation and remote memory updating, *Neuron*, **113** (2025), 471–485. https://doi.org/10.1016/j.neuron.2024.11.010

13. D. Osorio-Gómez, M. I. Miranda, K. Guzmán-Ramos, F. Bermúdez-Rattoni, Transforming experiences: Neurobiology of memory updating/editing, *Front. Syst. Neurosci.*, **17** (2023), 1103770. https://doi.org/10.3389/fnsys.2023.1103770

14. C. Wang, H. Yue, Z. Hu, Y. Shen, J. Ma, J. Li, et al., Microglia mediate forgetting via complement-dependent synaptic elimination, *Science*, **367** (2020), 688–694. https://doi.org/10.1126/science.aaz2288

15. J. Ruzicka, M. Dalecka, K. Safrankova, D. Peretti, P. Jendelova, J. C. F. Kwok, et al., Perineuronal nets affect memory and learning after synapse withdrawal, *Transl. Psychiatry*, **12** (2022), 480. https://doi.org/10.1038/s41398-022-02226-z

16. N. J. Mandelberg, R. Tsien, Weakening synapses to cull memories, *Science*, **363** (2019), 31–32. https://doi.org/10.1126/science.aaw1675

17. R. Fukaya, R. Miyano, H. Hirai, T. Sakaba, Mechanistic insights into cAMP-mediated presynaptic potentiation at hippocampal mossy fiber synapses, *Front. Cell. Neurosci.*, **17** (2023), 1237589. https://doi.org/10.3389/fncel.2023.1237589

18. K. Isler, C. P. van Schaik, Metabolic costs of brain size evolution, *Biol. Lett.*, **2** (2006), 557–560. https://doi.org/10.1098/rsbl.2006.0538

19. E. Bullmore, O. Sporns, The economy of brain network organization, *Nat. Rev. Neurosci.*, **13** (2012), 336–349. https://doi.org/10.1038/nrn3214

20. Q. She, G. Chen, R. Chan, Evaluating the small-world-ness of a sampled network: Functional connectivity of entorhinal-hippocampal circuitry, *Sci. Rep.*, **6** (2016), 21468. https://doi.org/10.1038/srep21468

21. S. Muldoon, E. Bridgeford, D. Bassett, Small-world propensity and weighted brain networks, *Sci. Rep.*, **6** (2016), 22057. https://doi.org/10.1038/srep22057

22. P. Taylor, Y. Wang, M. Kaiser, Within brain area tractography suggests local modularity using high resolution connectomics, *Sci. Rep.*, **7** (2017), 39859. https://doi.org/10.1038/srep39859

23. M. P. van den Heuvel, O. Sporns, Network hubs in the human brain, *Trends Cognit. Sci.*, **17** (2013), 683–696. https://doi.org/10.1016/j.tics.2013.09.012

24. O. Sporns, Structure and function of complex brain networks, *Dialogues Clin. Neurosci.*, **15** (2013), 247–262. https://doi.org/10.31887/DCNS.2013.15.3/osporns

25. A. Hahn, M. Breakspear, L. Rischka, W. Wadsak, G. M. Godbersen, V. Pichler, et al., Reconfiguration of functional brain networks and metabolic cost converge during task performance, *eLife*, **9** (2020), e52443. https://doi.org/10.7554/eLife.52443

26. L. K. Gallos, H. A. Makse, M. Sigman, A small world of weak ties provides optimal global integration of self-similar modules in functional brain networks, *Proc. Natl. Acad. Sci. U.S.A.*, **109** (2012), 2825–2830. https://doi.org/10.1073/pnas.1106612109

27. L. Yang, H. H. Zhang, Z. K. Sun, L. Du, G. R. Chen, Hippocampal CA3–CA1 synaptic network model of memory, *Nonlinear Dyn.*, **112** (2024), 7499–7525. https://doi.org/10.1007/s11071-024-09375-4

28. L. Yang, H. H. Zhang, Z. K. Sun, Hippocampus encoding memory engrams as stable heteroclinic network, *Chaos*, **34** (2024), 123118. https://doi.org/10.1063/5.0223045

29. L. Yang, H. H. Zhang, Z. K. Sun, Modeling dynamics of memory integration and retrieval in the hippocampus, *Eur. Phys. J. Spec. Top.*, **2025** (2025). https://doi.org/10.1140/epjs/s11734-025-01821-7

30. T. D. Shou, *Neurobiology*, 3nd edition (in Chinese), Beijing: Higher Education Press, 2013.

31. A. Guet-McCreight, F. K. Skinner, L. Topolnik, Common principles in functional organization of VIP/calretinin cell-driven disinhibitory circuits across cortical areas, *Front. Neural Circuits*, **14** (2020), 32. https://doi.org/10.3389/fncir.2020.00032

32. E. Abs, R. B. Poorthuis, D. Apelblat, K. Muhammad, M. B. Pardi, L. Enke, et al., Learning-related plasticity in dendrite-targeting layer 1 interneurons, *Neuron*, **100** (2018), 684–699. https://doi.org/10.1016/j.neuron.2018.09.001

33. Z. Kohus, S. Káli, L. Rovira-Esteban, D. Schlingloff, O. Papp, T. F. Freund, et al., Properties and dynamics of inhibitory synaptic communication within the CA3 microcircuits of pyramidal cells and interneurons expressing parvalbumin or cholecystokinin, *J. Physiol.*, **594** (2016), 3745–3774. https://doi.org/10.1113/JP272231

34. R. Evangelista, G. Cano, C. Cooper, D. Schmitz, N. Maier, R. Kempter, Generation of sharp wave-ripple events by disinhibition, *J. Neurosci.*, **40** (2020), 7811–7836. https://doi.org/10.1523/JNEUROSCI.2174-19.2020

35. B. Dudok, P. M. Klein, E. Hwaun, B. R. Lee, Z. Yao, O. Fong, et al., Alternating sources of perisomatic inhibition during behavior, *Neuron*, **109** (2021), 997–1012. https://doi.org/10.1016/j.neuron.2021.01.003

36. M. Udakis, V. Pedrosa, S. E. L. Chamberlain, C. Clopath, J. R. Mellor, Interneuron-specific plasticity at parvalbumin and somatostatin inhibitory synapses onto CA1 pyramidal neurons shapes hippocampal output, *Nat. Commun.*, **11** (2020), 4395. https://doi.org/10.1038/s41467-020-18074-8

37. T. Jing, L. Yang, W. G. Sun, Exact calculations of network coherence in weighted ring-trees networks and recursive trees, *Phys. Scr.*, **96** (2021), 085217. https://doi.org/10.1088/1402-4896/ac0277

38. J. Chen, L. Zhou, W. G. Sun, Consensus analysis of chain star networks coupled by leaf nodes, *Phys. Scr.*, **98** (2023), 125204. https://doi.org/10.1088/1402-4896/ad0588

39. A. J. DeCostanzo, C. C. A. Fung, T. Fukai, Hippocampal neurogenesis reduces the dimensionality of sparsely coded representations to enhance memory encoding, *Front. Comput. Neurosci.*, **12** (2019), 99. https://doi.org/10.3389/fncom.2018.00099

40. P. Rao-Ruiz, E. Visser, M. Mitrić, A. B. Smit, M. C. van den Oever, A synaptic framework for the persistence of memory engrams, *Front. Synaptic Neurosci.*, **13** (2021), 661476. https://doi.org/10.3389/fnsyn.2021.661476

41. K. M. Swallow, J. M. Zacks, R. A. Abrams, Event boundaries in perception affect memory encoding and updating, *J. Exp. Psychol. Gen.*, **138** (2009), 236–257. https://doi.org/10.1037/a0015631

42. S. Tazerart, D. E. Mitchell, S. Miranda-Rottmann, R. Araya, A spike-timing-dependent plasticity rule for dendritic spines, *Nat. Commun.*, **11** (2020), 4276. https://doi.org/10.1038/s41467-020-17861-7

AIMS Press